INSTITUTO TECNOLOGICO Y DE ESTUDIOS SUPERIORES DE MONTERREY

CAMPUS MONTERREY

Model for Photonic Packet-Switched Networks with Bursty Traffic Project

Master of Science in Electronic Engineering Major in Telecommunications

by

Ing. Job Josué Constantino Prado 785781

December 2003

Contents

1 Abstract

A detailed analytical traffic model for all-optical wavelength division multiplexing (WDM) photonic packet-switched router is presented and the requirements for buffer size are analyzed. Also it is known that due to the topology, packets may generate traffic bottlenecks produced by a tendency of the routing scheme to send packets with different destinations through preferred paths. This effect increases the traffic load and, hence, the probability of blocking at the output links of specific routers in the network and, therefore, a large buffer depth is required or an increment in the number of fibers per link. Furthermore, the relationship between traffic features at optical level and node modelling is addressed in order to outline analytical models to assess node performance. An analytical representation of traffic correlation, alongside with forwarding and buffering at switching nodes is discussed in order to support performance assessments such as packet loss probability. The statistical features, e.g. marginal distribution and correlation structure, of traffic reaching an output buffer in a time-slotted photonic packet switching node is investigated. Packet arrival patterns are generated through a well-known on-off analytical model with short-range dependence that accounts for packet forwarding as well. The purpose here is to find out how far the analytical model is from representing relevant characteristics present in self-similar traffic traces. An approach is proposed for modelling buffers under bursty traffic.

2 Introduction

We focus on a fully optical network, which considers correlated traffic, as can be found on Ethernet traces, as self-similar traffic, instead of just independent traffic, we only consider an isolated node.

We analyze traffic features of an optical node, which uses WDM-Wavelength Division Multiplexing and has a partitioned buffer, one per outlet, as method for solving blocking experimented by packets when they try to get the same outlet. An analytical representation of traffic correlation, alongside with forwarding and buffering at switching nodes is discussed in order to support performance assessments such as packet loss probability, through the analysis of marginal distribution and correlation structure, of traffic reaching an output buffer in a time-slotted photonic packet switching node.

Packet arrival patterns are generated through a on-off analytical model with short-range dependence that accounts for packet forwarding as well.

The analysis of performance when the traffic finally goes through buffers and modelling buffers under bursty traffic, is the main matter of study.

1 Abstract

A detailed analytical traffic model for all-optical wavelength division multiplexing (WDM) photonic packet-switched router is presented and the requirements for buffer size are analyzed. Also it is known that due to the topology, packets may generate traffic bottlenecks produced by a tendency of the routing scheme to send packets with different destinations through preferred paths. This effect increases the traffic load and, hence, the probability of blocking at the output links of specific routers in the network and, therefore, a large buffer depth is required or an increment in the number of fibers per link. Furthermore, the relationship between traffic features at optical level and node modelling is addressed in order to outline analytical models to assess node performance. An analytical representation of traffic correlation, alongside with forwarding and buffering at switching nodes is discussed in order to support performance assessments such as packet loss probability. The statistical features, e.g. marginal distribution and correlation structure, of traffic reaching an output buffer in a time-slotted photonic packet switching node is investigated. Packet arrival patterns are generated through a well-known on-off analytical model with short-range dependence that accounts for packet forwarding as well. The purpose here is to find out how far the analytical model is from representing relevant characteristics present in self-similar traffic traces. An approach is proposed for modelling buffers under bursty traffic.

2 Introduction

We focus on a fully optical network, which considers correlated traffic, as can be found on Ethernet traces, as self-similar traffic, instead of just independent traffic, we only consider an isolated node.

We analyze traffic features of an optical node, which uses WDM-Wavelength Division Multiplexing and has a partitioned buffer, one per outlet, as method for solving blocking experimented by packets when they try to get the same outlet. An analytical representation of traffic correlation, alongside with forwarding and buffering at switching nodes is discussed in order to support performance assessments such as packet loss probability, through the analysis of marginal distribution and correlation structure, of traffic reaching an output buffer in a time-slotted photonic packet switching node.

Packet arrival patterns are generated through a on-off analytical model with short-range dependence that accounts for packet forwarding as well.

The analysis of performance when the traffic finally goes through buffers and modelling buffers under bursty traffic, is the main matter of study.

3 Objective

Develop an optical router operating model.

- to model traffic generation and understand the traffic features reaching an output node. The traffic in this case is composed by sections of traffic coming from N inputs (each of them bearing n wavelengths) that are forwarded to the observed output. The analysis will be focused on any one particular output line.
- to assess the effectiveness of buffering under both uncorrelated and correlated traffic.

4 Justification

Router traffic models have already been covered considering independent traffic (packets), here is wanted to solve the same situation considering correlated traffic, which is not available yet in scientific literature. The idea that routers analyzed be optical is due to there is no need to electronic conversion. That is what we expect for reducing costs in network and for explotation of optical transparency (to transmission bitrate) . All optical networks is expected to be in use during next future and this model will have direct applications to those networks, giving a really useful model.

5 Routing scheme and router architecture

Optical packets must be routed through a network from the origin and through intermediate nodes (OXCN) to reach the destination. The general optical WDM network which we consider is shown in Fig. 1. It is a mesh network in which signals on n different wavelengths, $\lambda_1 ... \lambda_n$, are used to carry cell traffic between the optical network nodes.

Wavelength division multiplexing (WDM) has been proposed as a way of increasing the capacity in future optical networks. Furthermore, WDM networks are likely to use optical switching to avoid the bottlenecks of electronics as well as to increase the transparency of optical networks. The absence of an effective way to store cells in the optical domain, reduces the realistic buffer capacity of optical packet switches. The optical buffer is realized by fiber delay-lines. By exploiting the wavelength dimension by using WDM and employing tuneable optical wavelength converters (TOWC's), the required number of fiber delay-lines in optical packet switches can be reduced.

3 Objective

Develop an optical router operating model.

- to model traffic generation and understand the traffic features reaching an output node. The traffic in this case is composed by sections of traffic coming from N inputs (each of them bearing n wavelengths) that are forwarded to the observed output. The analysis will be focused on any one particular output line.
- to assess the effectiveness of buffering under both uncorrelated and correlated traffic.

4 Justification

Router traffic models have already been covered considering independent traffic (packets), here is wanted to solve the same situation considering correlated traffic, which is not available yet in scientific literature. The idea that routers analyzed be optical is due to there is no need to electronic conversion. That is what we expect for reducing costs in network and for explotation of optical transparency (to transmission bitrate) . All optical networks is expected to be in use during next future and this model will have direct applications to those networks, giving a really useful model.

5 Routing scheme and router architecture

Optical packets must be routed through a network from the origin and through intermediate nodes (OXCN) to reach the destination. The general optical WDM network which we consider is shown in Fig. 1. It is a mesh network in which signals on n different wavelengths, $\lambda_1 ... \lambda_n$, are used to carry cell traffic between the optical network nodes.

Wavelength division multiplexing (WDM) has been proposed as a way of increasing the capacity in future optical networks. Furthermore, WDM networks are likely to use optical switching to avoid the bottlenecks of electronics as well as to increase the transparency of optical networks. The absence of an effective way to store cells in the optical domain, reduces the realistic buffer capacity of optical packet switches. The optical buffer is realized by fiber delay-lines. By exploiting the wavelength dimension by using WDM and employing tuneable optical wavelength converters (TOWC's), the required number of fiber delay-lines in optical packet switches can be reduced.

3 Objective

Develop an optical router operating model.

- to model traffic generation and understand the traffic features reaching an output node. The traffic in this case is composed by sections of traffic coming from N inputs (each of them bearing n wavelengths) that are forwarded to the observed output. The analysis will be focused on any one particular output line.
- to assess the effectiveness of buffering under both uncorrelated and correlated traffic.

4 Justification

Router traffic models have already been covered considering independent traffic (packets), here is wanted to solve the same situation considering correlated traffic, which is not available yet in scientific literature. The idea that routers analyzed be optical is due to there is no need to electronic conversion. That is what we expect for reducing costs in network and for explotation of optical transparency (to transmission bitrate) . All optical networks is expected to be in use during next future and this model will have direct applications to those networks, giving a really useful model.

5 Routing scheme and router architecture

Optical packets must be routed through a network from the origin and through intermediate nodes (OXCN) to reach the destination. The general optical WDM network which we consider is shown in Fig. 1. It is a mesh network in which signals on n different wavelengths, $\lambda_1 ... \lambda_n$, are used to carry cell traffic between the optical network nodes.

Wavelength division multiplexing (WDM) has been proposed as a way of increasing the capacity in future optical networks. Furthermore, WDM networks are likely to use optical switching to avoid the bottlenecks of electronics as well as to increase the transparency of optical networks. The absence of an effective way to store cells in the optical domain, reduces the realistic buffer capacity of optical packet switches. The optical buffer is realized by fiber delay-lines. By exploiting the wavelength dimension by using WDM and employing tuneable optical wavelength converters (TOWC's), the required number of fiber delay-lines in optical packet switches can be reduced.

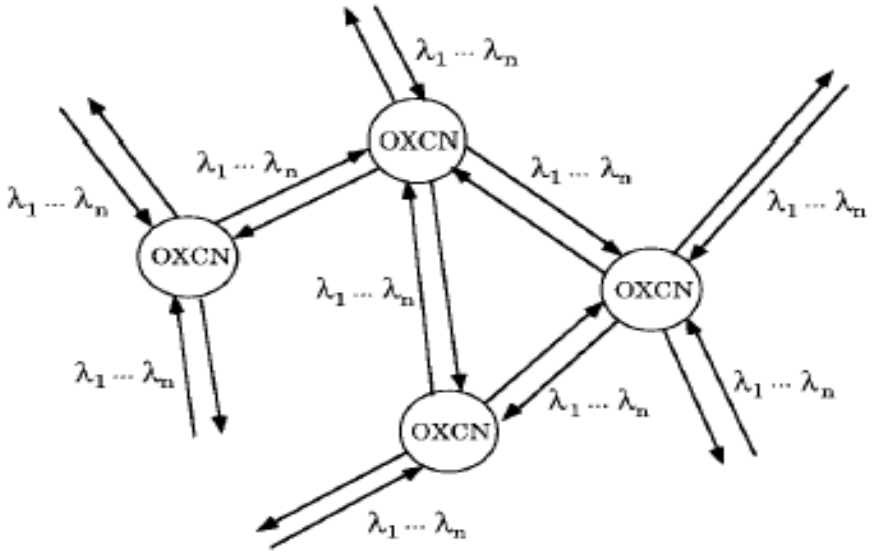

Figure 1: WDM WAN Backbone Network.

The decision of the path to be followed is made by a control unit, which most often is implemented with electronic techniques. The routing algorithm is closely related to the network topology and, thus, to the type of switching routers in use. Routers in irregular meshed networks use predefined lookup tables to forward- arriving packets. Usually, a shortest path or least number of hops algorithm is used to define the optimum output at every router in the network. There is normally a single path and, therefore, one output for every packet that arrives to the router. Analysis of the router performance in terms of packet loss, number of delay lines, size of the router, and number of wavelengths has been studied for the case of single-path routing and uniform-router traffic [3]. The router architecture, demonstrated in [4], is the architecture used in this analysis and is shown in Fig. 2.

The demultiplexer (DEMUX) selects the packets arriving on wavelengths $\lambda_1, ..., \lambda_n$, on each of the N input fibers. Optical- to-electrical interfaces located after the DEMUX are used to read the packet headers by which the destination and thereby switch outlet can be found. Also, after the demultiplexer, tunable WCs are utilized to solve blocking of packets by addressing free space in the fiber delay-line output buffers. The space switch consists of optical gates that control the flow of packets to the designated output and fiber-delay lines in the output buffer, the size of the space switch is $Nxn \cdot N(B/n)$. Fiber-delay lines provide the packet buffering and are present at the output of the router [3]. In Fig. 2, B is the number of cell positions in the buffer, n is the number os wavelengths, N the number of in- and out-lets and B/n the number of fiber-delay lines, each capable of storing n packets. There is at least one inlet to inject up to n packets into the network and at least one outlet to absorb up to n packets from the network. Logically, the router has the functions of packet dropping (absorption), adding (injection), wavelength switching (conversion), routing (space switch), and buffering. Observe that architecture in Fig. 2 has completely partitioned buffers because fiber-delay lines are distributed among the outlets.

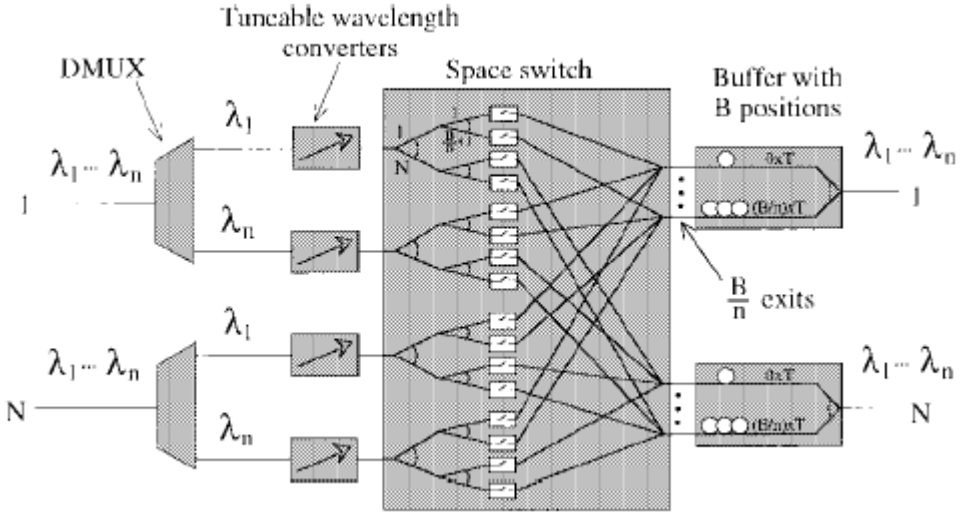

Figure 2: WDM packet switch with buffers realized as fiber delay-lines and with tuneable wavelength converters to address free space in the buffers. T corresponds to the duration of a packet.

In Fig. 3 we see the physical layout of fiber delay-line buffer architecture. Architectures with buffers dedicated to each outlet require a smaller number of wavelengths in comparison to shared buffers. Efforts must be gathered towards understanding traffic features in order to keep the buffer depth as low as possible. Noise accumulation, power splitting, fibre non-linearities, crosstalk, amplitude and phase fluctuation in the switch fabric are some of degrading effects taking place at physical layer. The performed analysis here considered does not take into account influences of physical layer on packet loss performance.

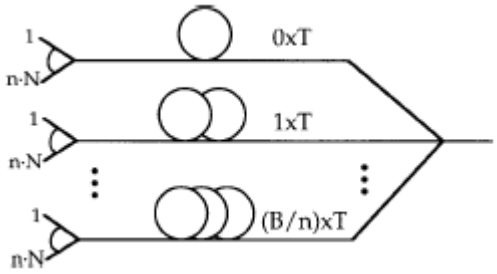

Figure 3: Physical layout of fiber delay-line buffer architecture. B is the number of cell positions in the buffer, n the number of wavelength channels per in- and out-let, N is the number of physical in- and out-lets while T is the duration of a cell.

6 Traffic of packets at electronic layers

Teletraffic theory is being changed to a great extend during the last decades. It is often argued that models that were extensively used in telephony do not account for features of todays data-oriented network. Telephony network uses circuit-switched technology and traffic is basically modelled as Poisson arrivals (connection requests) and exponential holding time per connections; leading to what is called Erlang distribution for blocking probability when establishing a new connection [6]. Hence, one is able to properly design network elements that are to be shared by many subscribers, e.g. switching centres modules and trunk lines. In packet switched networks, on the other hand, the aim is to design buffers with the purpose of reaching an acceptable packet loss probability by solving packet contention.

Temporal correlation between packets has been one of salient feature present throughout the history of packet switching technology. The first efforts to model the bursty behaviour of data networks let to the concept of packet trains discussed in [10]. Comprehensive statistical characterisation studies were pursued in [11] until a major breakthrough happened in early 90s when Long-Range Dependence (LRD), also known as self-similarity, has been identified in Ethernet traffic [5]. Self-similarity could be summarised as follows. The observation of traffic sources indicates a very large variance associated to the amount of traffic generated. In addition, this traffic possesses high levels of time-correlation spreading across long periods. Consequently, the effectiveness of buffering in reducing packet loss (due to contention) is considerably weakened and so is the aggregation at the core network of the photonic router as a means of smoothing traffic variance and improving link utilisation.

6.1 Causes of long-range dependence

In voice connections generally one part speaks while the other remains mute. Therefore, the production of packets is a clear alternation between bursty and silent periods. It is perfectly foreseeable that this dependence is expected, on average, not to last for very long time span once it is due to the bursty nature of human conversation itself. This leads to temporal-correlation among generated packets that, in contrast with voice over packets, may persist over very long periods of time.

6.2 Traffic features

The statistical background to understand the features of modern traffic sources is briefly discussed here. It has two basic objectives: to clarify the relevant issues on traffic characterization, and to introduce few basic mathematical tolls used for trace analysis in this work.

6.3 Section arrivals and duration, packet inter-arrival time, arrival counting, and heavytailness

Arrival of section requests can be still modelled as Poisson arrivals just like connection requests in telephony for human generated requests such as telnet and FTP [14]. However, sections time distribution on the Internet, whatever origin, presents slow decay. This contrasts with connection duration (holding time), well represented by exponential distribution in telephony. This sort of probability distribution is often called heavy-tail and is defined as in (1)

$$Prob\{U \geq u\} \approx u^{-\alpha} L(u) \text{ as } u \longrightarrow \infty \text{ and } \alpha > 0 \tag{1}$$

with $1 \leq \alpha \leq 2$ and L(u) being a slowly-varying function (e.g. logarithm or constant such as $lim_{t \longrightarrow \infty} L(tx)/L(t) = 1$). One may interpret (1) as follows: most connection lasts very little but the bulk of the traffic volume is composed by few long-living connections [12]. Another consequence of heavytailness associated to section duration is that the longer the period of observed activity, the more certain that it will persist into the future [13]. In light-tail distributed process (such as exponential) the expected duration is the same regardless of its elapsed time. The IP network is not slotted in time. As a result, some prefer to associate the high variability of heavy-tail distributions to the interval between arrivals (inter-arrival time). On the other hand, for ATM traffic, which works on a slotted-time basis, the variance is often related to the number of arrivals (or amount of bytes) in a multiple of the time-slot interval. Traffic will be regarded as a time-discrete stochastic process $X(t)$ comprising arrivals (e.g. bits, bytes or packets) per time interval. It must be said that the heavy-tail feature does not necessary imply self-similarity.

6.4 Stationarity

A discrete stochastic process $X(t)$ is considered stationary whenever its joint statistical features for any set of samples are all the same regardless of the time-reference frame adopted for observation. Under a less restrictive definition, if at least the two first moments are time-invariant, one may define the autocorrelation coefficient $r(k)$ as in (4), where $\mu_X = E[X]$ and $\sigma_X^2 = E[(X - \mu)^2]$ are the mean and variance respectively.

$$r(u, v) = E[(X_u - \mu)(X_v - \mu)]/\sigma_X^2 \tag{2}$$

$$r(u, v) = r(u + k, v + k) \qquad u, v, k \in \{0, 1, 2, ...\} \tag{3}$$

$$r(u, v) = r(0, u - v) = r(k) \tag{4}$$

If the autocorrelation function also satisfies the translation invariance, leading to the autocorrelation function being defined only by the relative difference between temporal samples as in (4), this process is classified as wide-sense stationary (also known as secondorder stationarity) [6].

6.5 Long-range dependence and second-order self-similarity

A wide-sense stationary process $X(t)$ is long-range dependent (LRD) if $r(k)$ is non-sumable (i.e. $\sum_k |r(k)| \longrightarrow \infty$), meaning that samples are still related to each other no matter how far apart they are. An exact (second order) self-similar process is characterised by the Hurst factor H $(0.5 < H < 1)$ shown in (5) [9].

$$r(k) = \begin{cases} [(k+1)^{2H} - 2k^{2H} + (k-1)^{2H}] & 0 < k < \infty \\ 1 & k = 0 \end{cases} \tag{5}$$

Experimental measurements can be compared with (5) for identification of LRD in traces. For a finite number of samples, say Z, the correlation coefficient can be obtained as in (6)

$$\hat{r}(k) = \frac{\sum_{i=1}^{Z-k}[X(t_i - \hat{\mu}_X)][X(t_i - t_k) - \hat{\mu}_X]}{(Z-k)\hat{\sigma}_X^2} \tag{6}$$

where $\hat{\mu}_X$ and $\hat{\sigma}_X$ are temporal mean and (unbiased) variance estimation from the finite traffic trace calculated as shown in (7) [6]

$$\hat{\mu}_X = \frac{1}{Z}\sum_{i=1}^{Z} X(t_i) \qquad\qquad \hat{\sigma}_X^2 = \frac{1}{Z-1}\sum_{i=1}^{Z}[X(t_i) - \hat{\mu}_X]^2 \tag{7}$$

By increasing the observation window (time-scale) in which a stochastic process is analysed, one may see the effects of long-range dependence manifesting its graphical fractal-like behaviour. This is due to the slow reduction of variance as the process is viewed in coarser scales. A convenient way to assess this (and estimate the Hurst factor) is by constructing a new stochastic process comprising of non-overlapping blocks of $X(t)$ containing $m \in \{1, 2, ...\}$ samples as shown in (8).

$$X^{\{m\}} = \frac{1}{m}\sum_{i=tm-m+1}^{tm} X(i) \tag{8}$$

Each block produces a single sample by averaging m samples of the original process. This is somehow equivalent to observing $X(t)$ in a time scale that is m coarser than the original. Notice that $lim_{m\longrightarrow\infty} X^{\{m\}} = \mu_X$ consequently $\sigma^2_{X^{\{m\}}} \longrightarrow 0$ as m increases towards infinity. Plotting the new variance against the aggregation factor using a log-log scale, one can use the slope (S) for Hurst parameter estimation $\hat{H} = (S+2)/2$, although this method does not allow interval of confidence measurements. It is worth looking at the two extreme values for H, with $H \longrightarrow 0.5$ the variance of $X^{\{m\}}$ reduces at the same rate m increases, which actually means that the stochastic process is completely uncorrelated. This lack of correlation can be confirmed by the fact that in (5) where $r(k) = 0$ for $H = 0.5$ and $k > 1$, meaning that no self-similarity will be present as the time scale of observation is increased and the variance is quickly smoothed by aggregation. On the other hand, for $H \longrightarrow 1$ the variance stays virtually the same regardless of the aggregation factor m. This is explained by the autocorrelation $r(k) = 1, \forall k$. In summary, the aggregated version depends upon the correlation structure of the original samples. Therefore, long-range dependence implies (second order) self-similarity. In other words, if samples are strongly related to each other

the aggregation will result in a process very similar to the original one (at least the variance). This also explains the presence of self-similarity MANs and WANs since aggregation does little to decrease variance when sources bear long-range dependence.

6.6 Statistics for aggregation in time

Let $X(t)$ represent the evolution in time of the volume of incoming traffic. This stochastic process produces random variables X_1, X_2, ... when sampled at a given regular time-interval $t = t_1$, $t = t_2$ ... respectively. The aggregation of m samples so that $F = X_1 + X_2 + ...X_m$, produces a sample of $\Theta(t)$ which represents the evolution of the aggregated traffic, where m the number of time-intervals collected from the original stochastic process. The expectancy (ensemble average $E[.]$) of this aggregation is a straightforward multiplication, shown in (9), of the original expectancy by the number of samples that has been grouped regardless of statistical dependence [24].

$$E[\Theta] = mE[X] \tag{9}$$

However, the general calculation for variance, here represented by $Var[.]$, is given by the summation of the autocovariance matrix [7] composed of mxm elements, that is, the summation all combinations of m elements in the correlation coefficient, as stated in (10).

$$var[\Theta] = \sum Cov_{xx} = var[X] \sum_{u=1}^{m} \sum_{v=1}^{m} r(u, v) \tag{10}$$

If arrivals are uncorrelated, the correlation coefficients are null except for $u = v$. Therefore the variance grows linearly with m as $u = v$ is satisfied m times. In the case of a wide-sense stationary and exact (secondorder) self-similar process, one may use the autocorrelation function given in (5) and substitute it in (10). Realising that $r(u, v) = r(|u - v|)$ due to the wide-sense stationarity, the double summation produce m occurrences of zero, and $2(m - k)$ of each value of k ($k \in \{1, 2, ..., m - 1\}$), the time-aggregation variance is then calculated as in (11).

$$var[\Theta_i] = var[X_i]\{m + \sum_{k=1}^{m-1} (m - k)[(k + 1)^{2H} - 2k^{2H} + (k + 1)^{2H}]\} = var[X_i]m^{2H} \tag{11}$$

The simple relationship between variance and aggregation revealed by (11) is at the root of self-similar stochastic processes. An exact (second-order) self-similar process proportionally maintains its variance, according to the Hurst factor, regardless of the observation interval. So, it is shown the equivalence of (10) and (11), named covariance matrix and self-similar property respectively, for an exact (second-order) self-similar process. Variance-plot performs gathering in time from the original trace but instead of simply collecting arrivals, variance-plots use a mean value, i.e. multiply the aggregate by $1/m$. As a result, the variance of new samples is the variance of the aggregate times $1/m^2$.

7 Model outlining

Performance estimation through mathematical models plays a central role in the design of present communication systems. The future photonic packet switching network will be no exception. However, a better understanding of traffic that will be processed by such nodes is still needed. The design of fundamental functions, e.g. contention resolution through buffering, depends upon this knowledge. It is often argued that traffic temporal correlation represented through models with Short-Range Dependence (SRD) is an obsolete method, since modern traffic sources actually possess long-range dependence (LRD) in their correlation structure. Nonetheless, one should seek a balance between simplicity and accuracy regarding the models utilized to represent the physical entities involved in the analysis of performance.

A simple illustration is given in Fig. 4 for the case analyzed in this work. The number of delay-lines provided to sort out contention is represented by b. Each wavelength (sometimes referred as channel in this work) is loaded at ρ ($0 \leq \rho \leq 1$) which can also be interpreted as the probability of finding a busy time-slot. Each source is assumed to have identical load. The major concerns of this project are:

- to model traffic generation and understand the traffic features reaching an output node. The traffic in this case is composed by sections of traffic coming from N inputs (each of them bearing n wavelengths) that are forwarded to the observed output. The analysis will be focused on any one particular output line.
- to assess the effectiveness of buffering under both uncorrelated and correlated traffic.

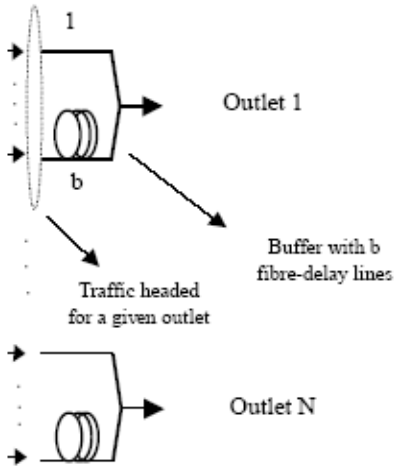

Figure 4: Illustration for output buffering and main issues discussed.

This project looks into traffic features of a simple model (bursty on-off) that is able to take into account correlation features at arrival and forwarding levels and is particularly suited for

output buffered nodes, like the one considered in this job. Marginal distribution, correlation structure, load distribution, and aggregation features are the characteristics studied via analysis and numerical simulation. Another point to be discussed here is to what extend claims that this sort of model overestimates node performance, due to the lack of LRD, are consistent. The detailed understanding developed here paves the way for performance assessment of nodes using output buffers under traffic with and without time correlation (and tuneable wavelength conversion). A well-known approach for modelling uncorrelated traffic buffering is initially presented to be generalized for the case of time-correlated arrival. If a given performance target is to be met, the traffic features and number of wavelengths utilized will dictate buffer depth which also affects switch matrix cross-point count as packets have to be directed to $b + 1$ elements in order to reach outlet without conflict.

8 Previous work

Analytical models representing traffic temporal-correlation with SRD have been in use since first investigations of voice over packets, e.g. [15] [16]. After the introduction of Asynchronous Transfer Mode (ATM) technology, these models have been extensively studied and upgraded in the view of new traffic sources bearing temporal correlation using this multimedia-oriented transport platform. There are two basic areas of study regarding the analytical model in this area. The first concerns the modelling of traffic sources themselves while the second addresses the transit and buffering of packets in switching nodes, involving the understanding of traffic gathering at outlets due to packet forwarding process and its influence on buffering performance. Studies analyzing traffic superposition of correlated sources can be found in [17], [18], and [19] while investigations into buffer performance are carried out in [2], [21], [1], and [20].

Photonic packet switching with fixed-size packets follows the footsteps of its electronic counterpart. Nevertheless, those traffic models used in ATM had to be modified to embrace particularities of photonic switching. The study presented in this work is based on model for source representation and traffic forwarding developed in [1] while buffer modelling and performance from [3], which is a generalisation from [21] for use of TWC/WDM. This work uses [2] to extend the model developed in [3] providing and exact and clear solution for performance evaluation of correlated traffic. Regardless of being a widely used model, little is known about traffic features produced by this method regarding the relevance of various factors that compose traffic statistics reaching output buffers. The validity of such a model when LRD is present, instead of SRD, needs to be assessed. The role played by both marginal distribution and correlation structure on buffer performance is yet not clear.

9 Model for packet source and forwarding

9.1 Source model

The model considers the input traffic per wavelength as a two-state system, more specifically High and Low for the representation used in Fig. 5.

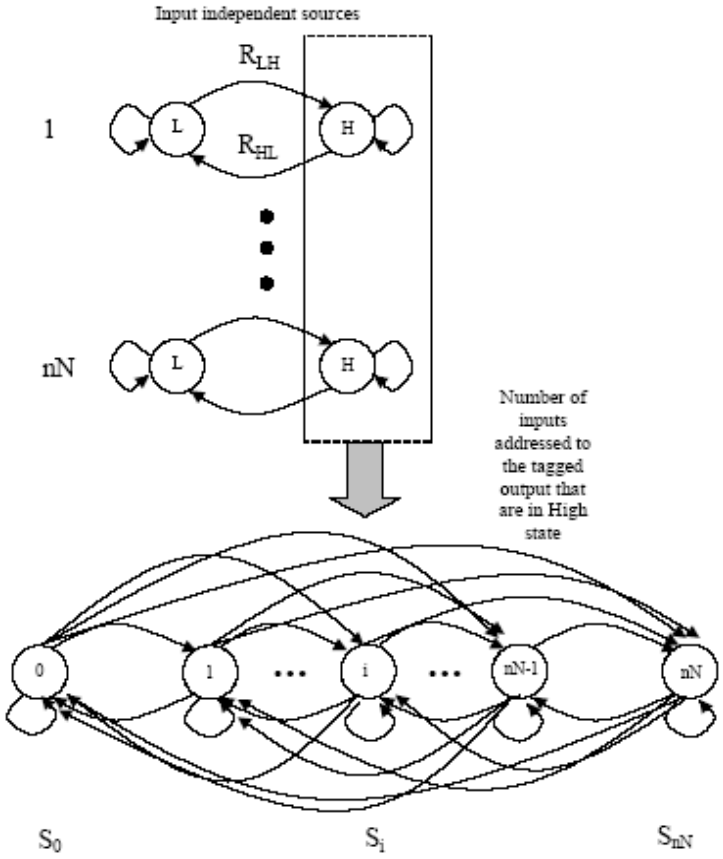

Figure 5: Analytical model. (a) Source representation.

Sources are independent and identically distributed (i.i.d.) and they are either producing a continuous stream of packets while in High state or no traffic at all during Low state. The transition probabilities R_{HL} and R_{LH} stand for High to Low and Low to High respectively. Each source spends, on average, $1/R_{LH}$ on Low state and $1/R_{HL}$ time-slots on High state. The latter is the mean burst length β, also known as burstiness. Applying local balance boundary to the source model shown in Fig. 5 one finds (12).

$$Prob[state = High] = R_{LH}/(R_{LH} + R_{HL}) \tag{12}$$

9.2 Forwarding model

Balanced input and output loads are assumed. The forwarding process considers that, in the long term, the incoming traffic is equally distributed among the output ports. An ingenious way is utilized in [1] to addresses forwarding via a hybrid representation between independent and correlated approaches. This is done by evenly distributing the input load among outputs in the long term but each burst generated is forwarded in a correlated way to a given output. Consequently, one only needs to keep track of sources addressed to the tagged output. As

packets are exclusively released in the High state, $Prob[state = High] = \rho/N$ and from (12) the probability of transition from Low to High can be calculated as stated in (13)

$$R_{LH} = \left(\frac{P}{N} R_{HL}\right) / \left(1 - \frac{P}{N}\right) \tag{13}$$

Temporal evolution for the number of sources in High state addressed to the tagged output is modelled by a Markov chain, illustrated in Fig. 5, in which any transition among the $S_i (0 \leq i \leq nN)$ states is allowed.

For each source, the transition probabilities are taken as geometric distributed with mean R_{HL} and R_{LH} for sources leaving state $H(ON)$ and state $L(OFF)$ respectively. As a result, the number of input sources in state H and addressed to the outlet under observation in a given timeslot is a binomial distribution, where i represents the current number of sources in High state while j also stands for that quantity a time-slot ahead. An auxiliary variable z is brought in to represent all possible combinations regarding transitions of individual sources, finally allowing the calculation of transition probability from i to j $(i, j \in \{0, 1, ..., nN\})$ in a compact expression [1] as shown (14).

$$Q_{ij} = Prob[S(T+1) = S_j \backslash S(T) = S_i] = \sum_{z=max(0,i-j)}^{min(i,nN-j)} \Delta L(z,i) \Delta H(z-i+j, nN-i)$$
$$\Delta_L(u,v) = \binom{v}{u} R_{HL}^u (1 - R_{HL})^{v-u}; \quad \Delta_H(u,v) = \binom{v}{u} R_{HL}^u (1 - R_{HL})^{v-u}$$

(14)

The resulting arrival pattern, represented here by a discrete stochastic process $A(t)$, at a given output is the summation of individual contributions in each time-slot as illustrated in Fig. 6 for three inputs that have packets addressed for the tagged outlet. The marginal distribution and two random variables from temporal samples of such a stochastic process A_τ and $A_{\tau+k}$, (taken at $t = \tau$ and $t = \tau + k$ respectively), are also shown.

10 Marginal distribution

Two methods for obtaining the marginal distribution for traffic reaching an output buffer are discussed here, namely, steady-state solution for the Markov chain representing state of input sources, and convolution of individual contributions within a time-slot.

10.1 Analysis via Markov chain

The steady-state solution for the temporal evolution of number of sources in High state can then be found by solving the equation system presented in (15). The underlined S and Q are the state

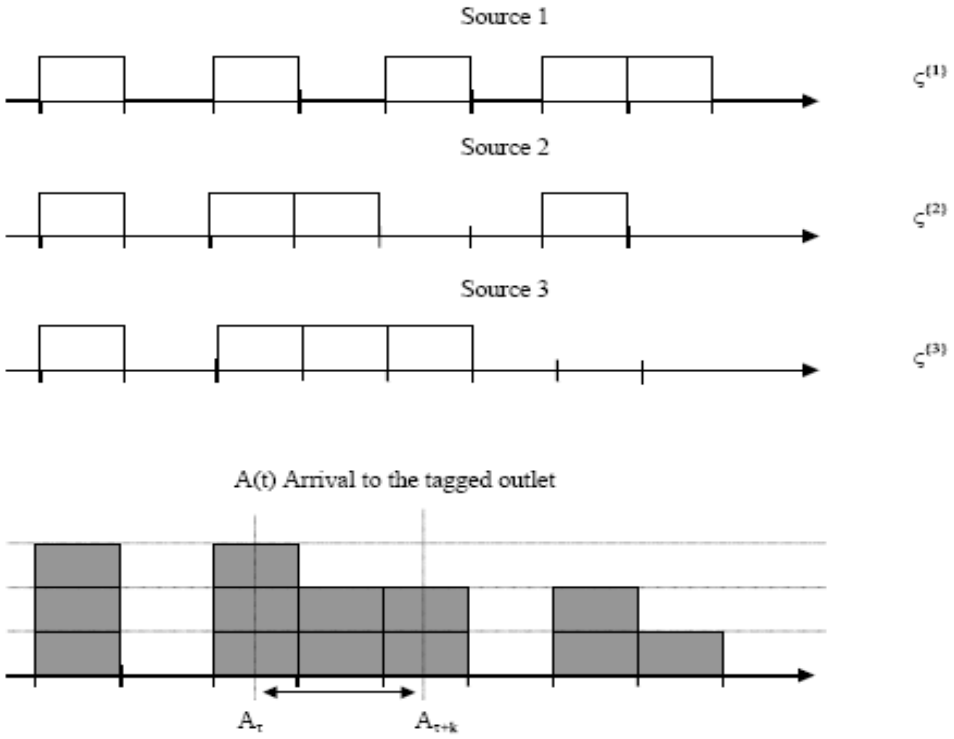

Figure 6: Analytical model. (b) Illustration for traffic reaching an output buffer.

and transition probabilities, in vector and matrix form respectively; e is a unitary column vector, i.e. $e = [11\ldots1]^T$, with $nN+1$ elements while $*$ stands for matrices product.

$$\begin{cases} \underline{S} = \underline{S} * \underline{\underline{Q}} \\ \underline{S} * \underline{e} = 1 \end{cases} \tag{15}$$

Once packets are released with probability 1 for sources at High state, vector S may be seen as the marginal distribution for the discrete-valued stochastic process A(t), i.e. $S = p_A(a) = Prob[A = a], a \in \{0, 1, 2, ..., nN\}$.

10.2 Analysis via Central Limit Theorem (CLT)

Provided that the traffic addressed to a given output is simply a summation of independent random variables $\varpi^{\{i\}}$, with $\varpi \in \{0, 1\}$ which are temporal samples from $\xi^{\{i\}}(t)$ coming from $i \in \{1, 2, ..., nN\}$ inputs within a time-slot as shown in Fig. 7, one is able to find out the marginal distribution at the outlet under analysis by convoluting the individual contributions from each input as stated in (16)

$$P_A(a) = P_\varsigma^{\{1\}}(\varpi) \otimes P_\varsigma^{\{2\}}(\varpi) \otimes \cdots \otimes P_\varsigma^{\{nN\}}(\varpi) \tag{16}$$

For the assumptions that have been made, the probabilities of sending either one or no packet to the tagged output is given by (17). One should expect this distribution to go through intermediate

profiles, e.g. Poisson-like, while with a limited number of sources before reaching Gaussian shapes for $nN \longrightarrow \infty$.

$$P_{\varsigma}(0) = Prob[\varpi = 0] = \left(1 - \frac{P}{N}\right); \quad P_{\varsigma}(1) = Prob[\varpi = 1] = \frac{P}{N} \tag{17}$$

Analysing CLT under balanced load presented and i.i.d. sources in (17) and (16) one can find (18).

$$P_A(a) = \binom{nN}{a} \left(\frac{P}{N}\right)^a \left(1 - \frac{P}{N}\right)^{nN-a} \tag{18}$$

Although the binomial distribution in (18) is widely used, e.g. [3] [21], calculations using (16) allow generalized cases, such as forwarding hot-spot, to be analyzed. Moreover, it provides a proof for the memoryless nature of the marginal distribution despite the presence of time correlation in each source composing the total arrivals.

11 Correlation structure

It is of great interest the correlation structure present in such aggregation of time-correlated but independent sources. An exact and simple method is developed to perform this investigation. In addition, an analytical calculation to obtain variance-plot charts is also introduced.

11.1 Correlation coefficient function

Provided that $A(t)$ is a stationary process, the two samples k time-slots apart, $k \in \{1, 2, ..., \infty\}$, A_0 and A_k, have the same marginal distribution $p_A(a)$ but they may not be independent. In order to evaluate the correlation coefficient between them, the joint probability density $p_{Ao,Ak}(a_o, a_k)$ is needed. Fig. 7 illustrates the relationship between time samples that is exploited in order to calculate the joint probability. The arrows represent transition probabilities given by (14).

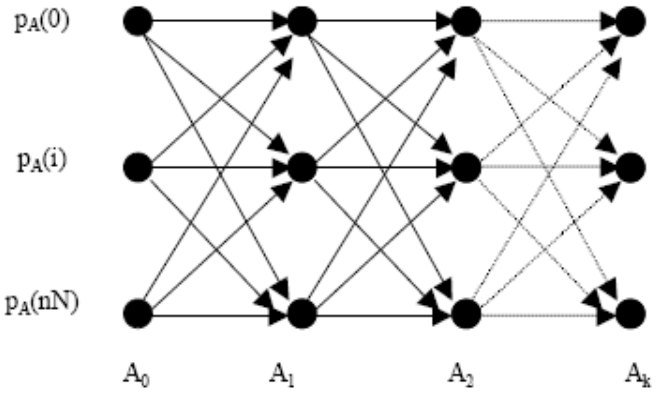

Figure 7: Correlation coefficient analytical calculations.

The joint density is then obtained by multiplying $p_A(a)$ by the conditional probabilities of transition (given by Q) for each step forward in time. If Q is stationary this may be represented as

in (19) where $(\cdot)$ stands for scalar product and pp is a square matrix composed $nN+1$ repetitions of $p_A(a)$, as shown in (20).

$$\underline{\underline{P_{A_1 A_k}}} = \underline{\underline{PP}} \cdot [\underline{\underline{Q}}(t_1 \backslash t_0)] * \cdots * \underline{\underline{Q}}(t_k \backslash t_{k-1})] = \underline{\underline{PP}} \cdot [\underline{\underline{Q}}]^k \tag{19}$$

$$\underline{\underline{\mathbf{PP}}} = \begin{bmatrix} \leftarrow & \underline{\underline{P_A}} & \rightarrow \\ & \vdots & \\ \leftarrow & \underline{\underline{P_A}} & \rightarrow \end{bmatrix} \tag{20}$$

Finally, the correlation coefficient can be found via covariance calculation [7], as stated by (21), where $E[.]$ represents the average over the ensemble.

$$r_A(k) = \frac{E[A_o, A_k] - E[A]^2}{E[A^2] - E[A]^2} \tag{21}$$

11.2 Traffic aggregation analysis for variance-plots

It is evident that an aggregated version of $A(t)$ directly depends upon the correlation structure of its original samples. Another way to see the aggregation process needed for variance-plots is as a summation of m correlated random variables, which is then multiplied by $1/m$ in order to obtain an averaged value over m samples. As a result, the analytically evaluated variance of $A[m]$, represented here by $Var(A[m]])$, is the variance of this gathering of m samples multiplied by $1/m_2$ as seen in (22).

$$Var[A^{[m]}] = \frac{1}{m^2} \sum_{u=1}^{m} \sum_{v=1}^{m} E[A_u, A_v] - E[A]^2 \tag{22}$$

In order to produce the variance plot required for H estimation, the variance obtained in (22) must be normalized by the initial variance ($m = 1$). Assuming that the stochastic process is wide-sense stationary, one obtains the normalized variance, $NV(m)$, as in (23).

$$NV(m) = \frac{Var[A^{[m]}]}{Var[A^{[1]}} = \frac{1}{m^2} \sum_{u=1}^{m} \sum_{v=1}^{m} r_A(u-v) = \frac{1}{m^2} \left[m + 2 \sum_{u=1}^{m-1} (m-u) r_A(u) \right] \tag{23}$$

Substituting the limits of correlation coefficient in (23), convergence to $1/m$ and 1 happens, as it would be expected, for uncorrelated and maximally correlated traffic respectively.

12 Model Evaluation

Traffic features generated by the model presented above (called here basic model with hybrid forwarding) are checked against numerical simulation. In addition, complex features, which are not included in the model such as correlated forwarding, is investigated to find out how they affect the traffic features at output buffers. Comparisons are performed in a framework that is generally used to analyze self-similar traffic. This is done in order to provide a clear judgement whether traffic features are underrepresented in the analytical model studied here. An ad hoc numerical simulator generates traces with 10^5 samples for a node with 16 ports and 4 wavelengths per fibre with the

purpose of validating the analytical study and providing some insight into the traffic features where analytical investigation would be rather complex. The offered load (ρ), from each 16x4 independent sources, is 0.8. A mean burst length (β) with 16 time-slots was chosen for the results presented.

12.1 Basic model with hybrid forwarding

For this case the offered load represented is actually 0.8=16, as seen in (18), due to the forwarding approach utilized. The marginal distribution is shown in Fig. 8 for both analytical and numerical models. It is also provided a Poisson density function with the same mean found in the trace. It is clear that the model generates Poisson-like densities for this node size and offered load. As expected, both methods for evaluating the marginal distribution produce the same result. This proves the number of active sources is a memoryless process.

Temporal correlation properties are exposed by autocorrelation function and aggregation analysis, shown in Fig. 9 and 10 respectively. However, Fig. 9 presents the autocorrelation obtained by the analytical procedure described in (19)-(21) and numerical evaluation of traces. It is evident the excellent agreement between them. One can observe in Fig. 9 that the correlation is negligible for lags over 60 time-slots. On the other hand, Fig. 10 shows that the variance for the aggregated version of this traffic remains virtually unchanged ($H = 0.96$) until the observation period exceeds the mean burst length (16 time-slots) then a steep reduction takes place as the trace becomes practically uncorrelated after that point. This is the explanation for the good fitting to a line to $H = 0.5$ shown by trace versions with aggregation factor larger than 56 time-slots. The best fitting for the whole range studied ($m = 1000$) would produce an estimated Hurst factor $H = 0.82$. However, when the autocorrelation function is also analyzed, it is easy to conclude that this is a meaningless result since traffic correlation present in this trace is short-range only. Nonetheless, it must be said that the trace has stronger correlation properties than an equivalent self-similar trace with $H = 0.82$ for lags below 29 time-slots. In this project, we are assuming that all outlinks are equally likely to be selected by inputlinks, but for considering imbalanced traffic, lector could see [20], [25] and [26].

13 Discussion

Once the model under analysis has proved to be accurate enough in representing important traffic features, issues related to performance assessment are now briefly discussed, allowing some important conclusion to be drawn regarding node performance evaluation.

13.1 Correlation span and performance

Before assessing buffer performance, one should carefully examine the traffic features reaching the buffer in order to better interpret outcomes of such experiments. The results presented in Fig. 11 are for summation of the correlation coefficients (from lags 1 to 100) against node size for different burstiness and offered load. This procedure is used here to obtain concise results regarding correlation behavior against all variables of the problem under analysis. A clear indication, provided by Fig. 11, is that little difference is to be expected from assessments of nodes size over 16 ports, as far as influence of correlation on performance is concerned. Lower levels of traffic produce higher levels of correlation. Less sensitive is the correlation to changes of node size for the case of low offered

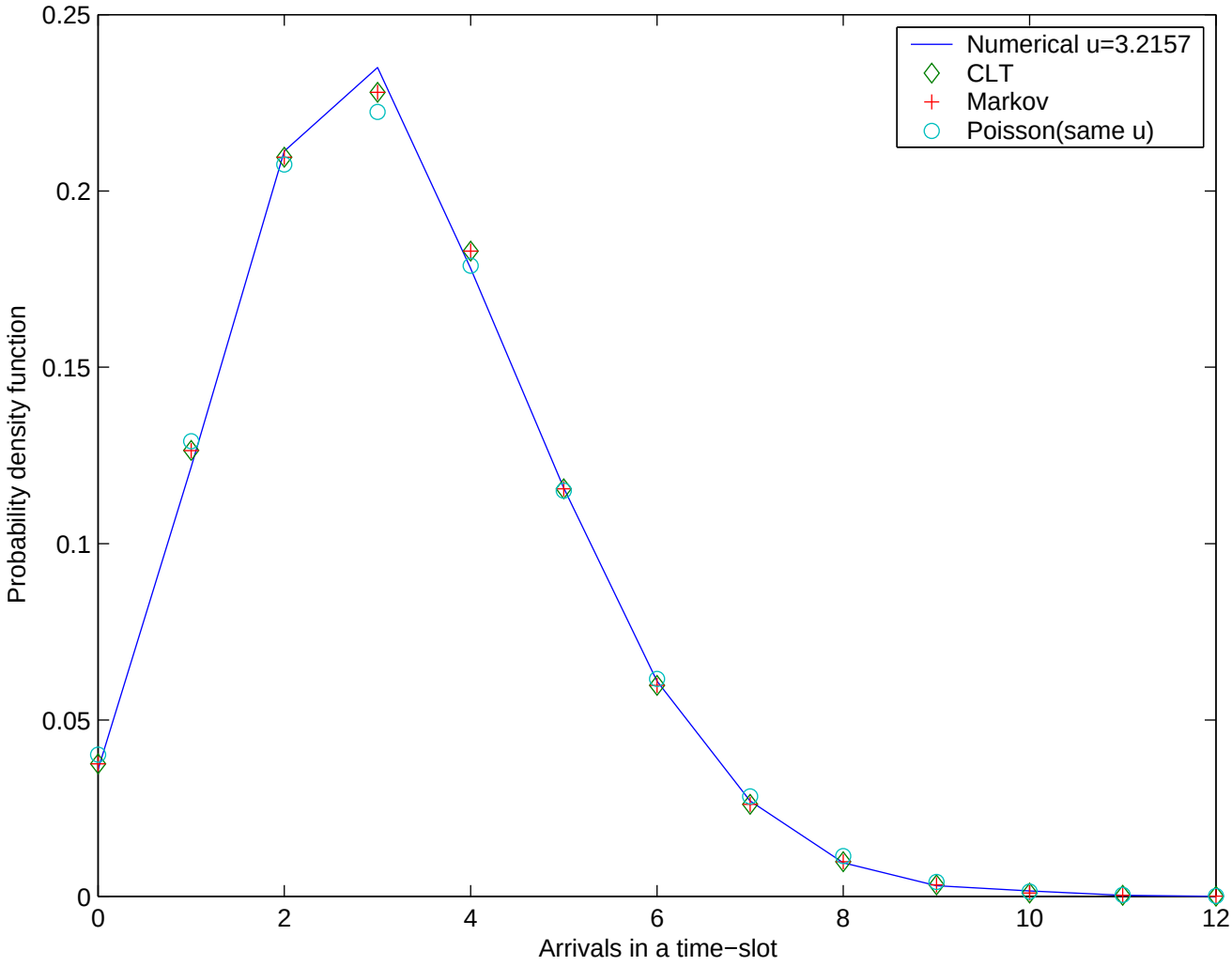

Figure 8: Model Evaluation: Marginal Distribution.

load. The higher the burstiness the wider the difference between curves for low and high offered load. Another important outcome is that the number of wavelengths (not shown) has virtually no impact on the results shown in Fig. 11.

Although it is clear that this traffic model only produces SRD, the correlation length is unbounded as Fig. 11 demonstrates when β is increased. Therefore, the inclusion of long-range dependence may only have minor importance in the context of the present study. More evidences to support this argument can be found in [22] and [23]. Moreover, the levels of short-range dependence match (or even exceed) the correlation levels from exact self-similar traffic within the range that might be realised by the optical buffer, as shown in Fig. 9 and 10.

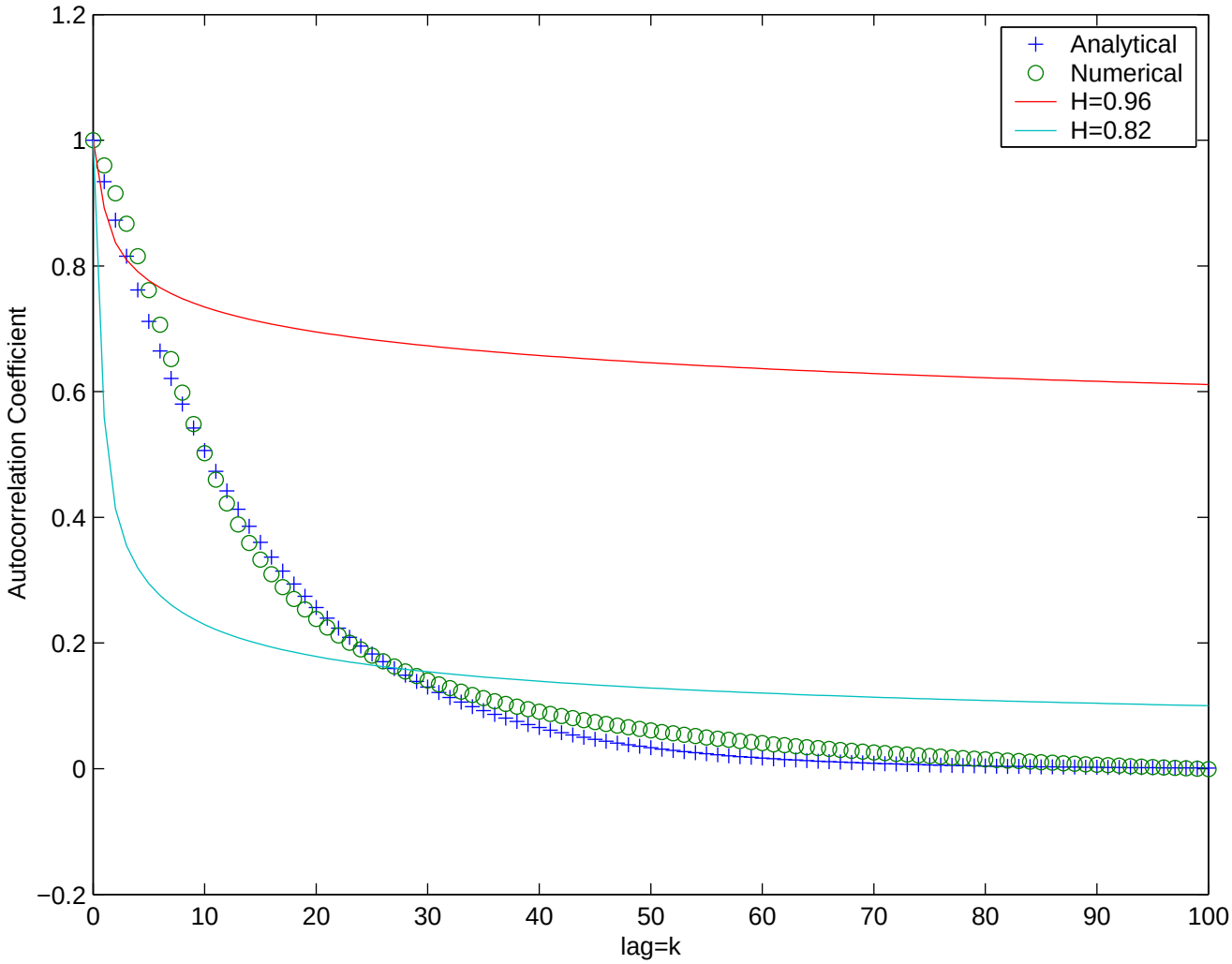

Figure 9: Model Evaluation: Autocorrelation.

14 Buffer performance under time-correlated traffic

The Markov chain representing the buffer state, should hold the number of inputs in High state [2], comprising therefore $(nN+1)x(B+1)$ elements as the vector holding the probability density for buffer occupancy demonstrates in (24).

$$\begin{array}{ccccc} \sum_{i=0}^{nN} q_{0i} = q_0 & & & & \sum_{i=0}^{nN} q_{Bi} = q_B \\ q = [\overbrace{q_{00} \cdots q_{0nN}} & \cdots & \cdots & & \overbrace{q_{B0} \cdots q_{BnN}}] \end{array} \tag{24}$$

The transition matrix between buffers states, now represented by $\underline{\underline{\Pi}}$, still has $(B+1)x(B+1)$ elements as shown in (25).

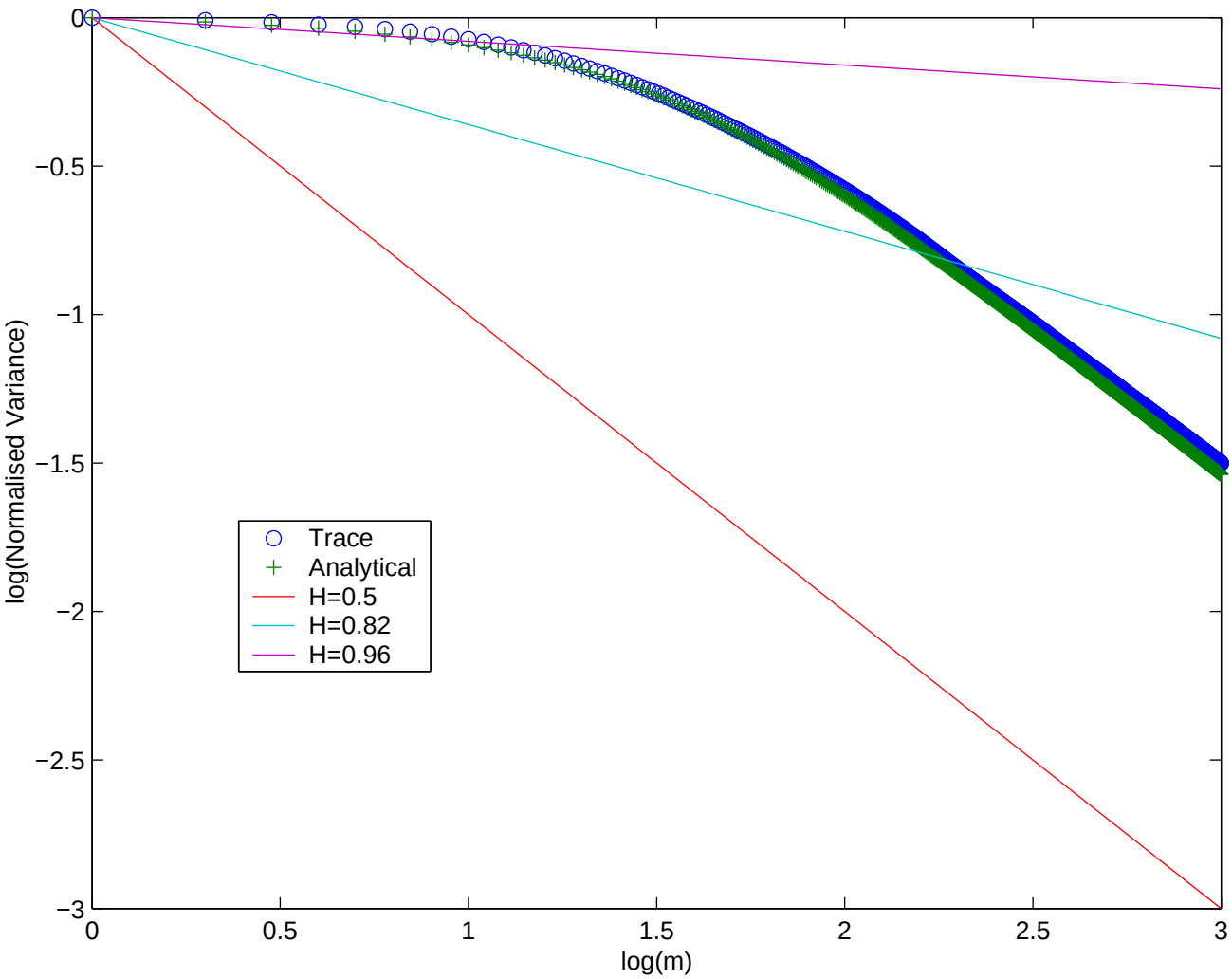

Figure 10: Model Evaluation: Variance-plot.

$$\underline{\underline{\mathbf{\Pi}}} = \begin{bmatrix} \underline{\underline{\pi_{0,0}}} & \cdots & \underline{\underline{\pi_{0,B}}} \\ \vdots & \ddots & \vdots \\ \underline{\underline{\pi_{B,0}}} & \cdots & \underline{\underline{\pi_{B,B}}} \end{bmatrix} \tag{25}$$

However, each element of this matrix is itself a sub-matrix with $(nN+1)x(nN+1)$ components [2]. This sub-matrix takes into account the transition among source states, as can be seen in (26).

$$\pi_{\mathbf{i,j}} = \begin{bmatrix} P_{ij}^{\{0\}} Q_{0,0} & \cdots & P_{ij}^{\{0\}} Q_{0,nN} \\ \vdots & \ddots & \vdots \\ P_{ij}^{\{nN\}} Q_{nN,0} & \cdots & P_{ij}^{\{nN\}} Q_{nN,nN} \end{bmatrix} \tag{26}$$

where Q_{mw} is the transition probability from m to w for the number of sources at ON state producing packets, and is given by (27)

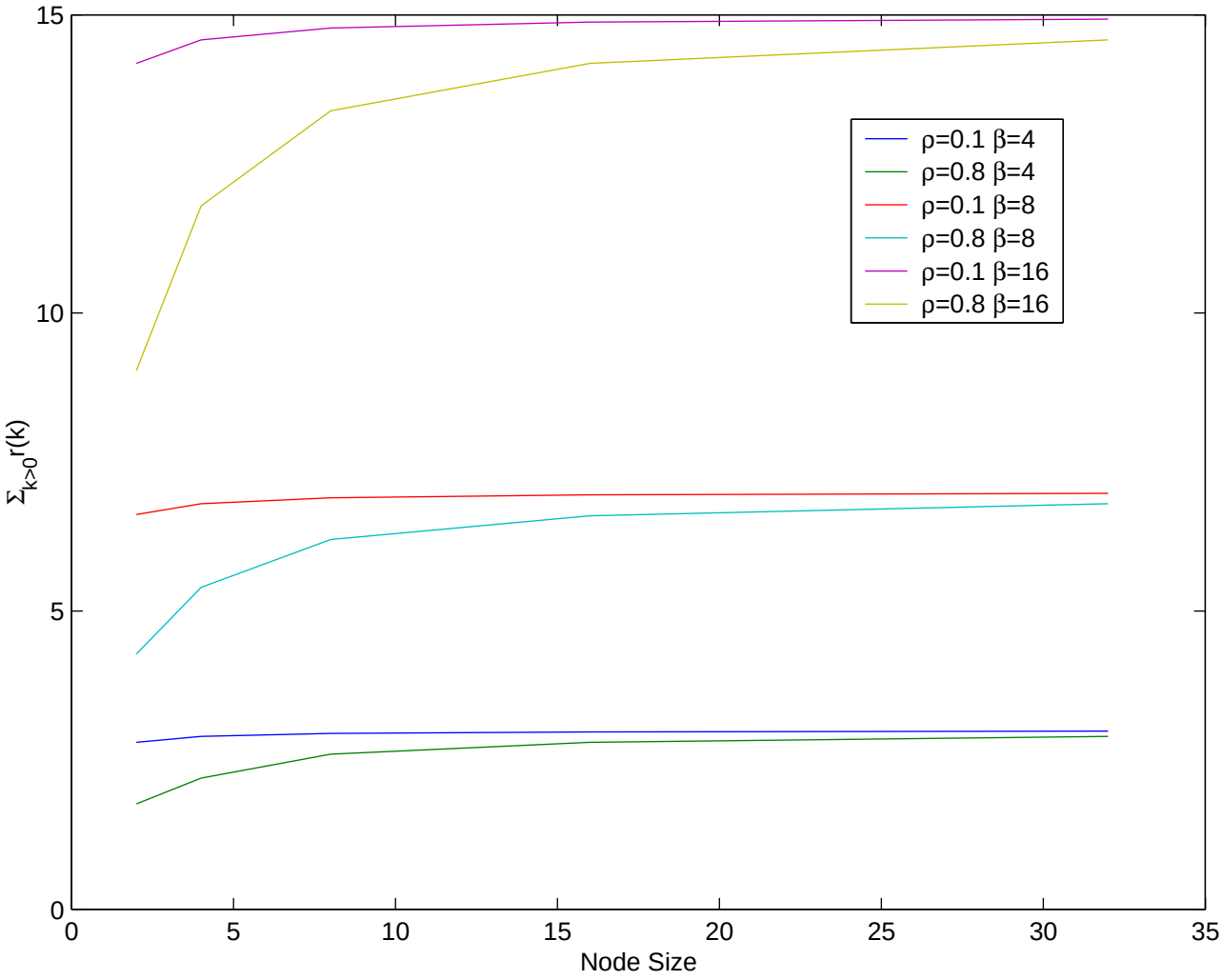

Figure 11: Summation over 100 time-slots for correlation coefficient.

$$Q_{mw} = \sum_{i=0}^{nN-m} \sum_{j=0}^{nN} T_m(i) S_m(j) \delta_{w,m-j+i} = \begin{cases} \sum_{j=m-w}^{min(m,nN-w)} T_m(w-m+j) S_m(j) \text{ if } m >= w \\ \sum_{i=w-m}^{min(w,nN-m)} T_m(i) S_m(m-w+i) \text{ if } m <= w \end{cases} \tag{27}$$

where $T_m(i)$ (or $S_m(j)$) represents the probability that i (or j) sources pass from the OFF state to the ON state (or viceversa), given that m of them are in ON state. Hence, we can see (28)

$$\begin{aligned} T_m(i) &= \binom{nN-m}{i} R_{LH}^i (1-R_{LH})^{nN-m-i} \\ S_m(j) &= \binom{m}{j} R_{HL}^j (1-R_{HL})^{m-j} \end{aligned} \tag{28}$$

The transition probabilities are shown in (29) but the number of sources in High state conditions the arrival probability.

$$P_{ij} = Prob[\Theta(T+1) = j \backslash \Theta(T) = i] = \begin{cases} \sum_{l=0}^{n-i} P_A(l) & 0 \le i \le n, j = 0 \\ P_A(j-i+n) & 0 \le i \le n, 1 \le j \le B-1 \\ P_A(j-i+n) & n+1 \le i \le B, i-n \le j \le B-1 \\ \sum_{l=B-i+n}^{nN} P_A(l) & 0 \le i \le B, j = B \\ 0 & \text{otherwise} \end{cases} \tag{29}$$

The probability of having i arrivals when c sources addressed to the tagged output are in High state can be straightforwardly represented by (30) since as the amount of packets released is deterministic once the number of active sources is set.

$$P_A^{\{c\}}(a) = P_A(a \setminus c) = \binom{c}{a} \mu_H^a (1-\mu_H)^{c-a},\ \mu_H = 1,\ \binom{c}{a} 0^{c-a} = \delta_{a,c} \tag{30}$$

The steady state solution for buffer occupancy is found in (31) where e is again a unitary column vector but in this case with $(nN+1)x(B+1)$ elements

$$\begin{cases} \underline{q} = \underline{q} * \underline{\underline{\Pi}} \\ \underline{q} * \underline{e} = 1 \end{cases} \tag{31}$$

Once q is found, the source states must be collapsed, as shown in (24), and therefore (32)-(34) can be applied in order to work out the packet loss probability for correlated traffic [3].

$$P_{0\lambda} = \sum_{i=0}^{n} \sum_{j=0}^{n-i} P_A(j) q_i \cdot [n - (i+j)] \tag{32}$$

$$NTP = \frac{n - p_{0\lambda}}{n} \tag{33}$$

$$PLP = 1 - \frac{NTP}{p} \tag{34}$$

Results in Fig. 12 investigate the influence of burstiness on efficiency of buffers in reducing packet loss probability for a load of 0.8.

It is clear the performance degradation due to the presence of time-correlation among arrivals. The slow decrease of packet loss versus buffer depth shows that even large buffers are not able to take the performance to reasonable values as temporal correlation increases. It can be seen that the offered load has little effect when the burstiness factor is high.

15 Conclusions

This model only assess performance metrics through on-off sources to generate the traffic, guiding to evaluate only short-range dependence, since this are memory-less processes. Performance degradation is noticed when correlation increases in the router traffic, demanding more resources in order to maintain a specific packet loss probability, with respect to independent traffic. When burstiness increases, performance is hardly affected.

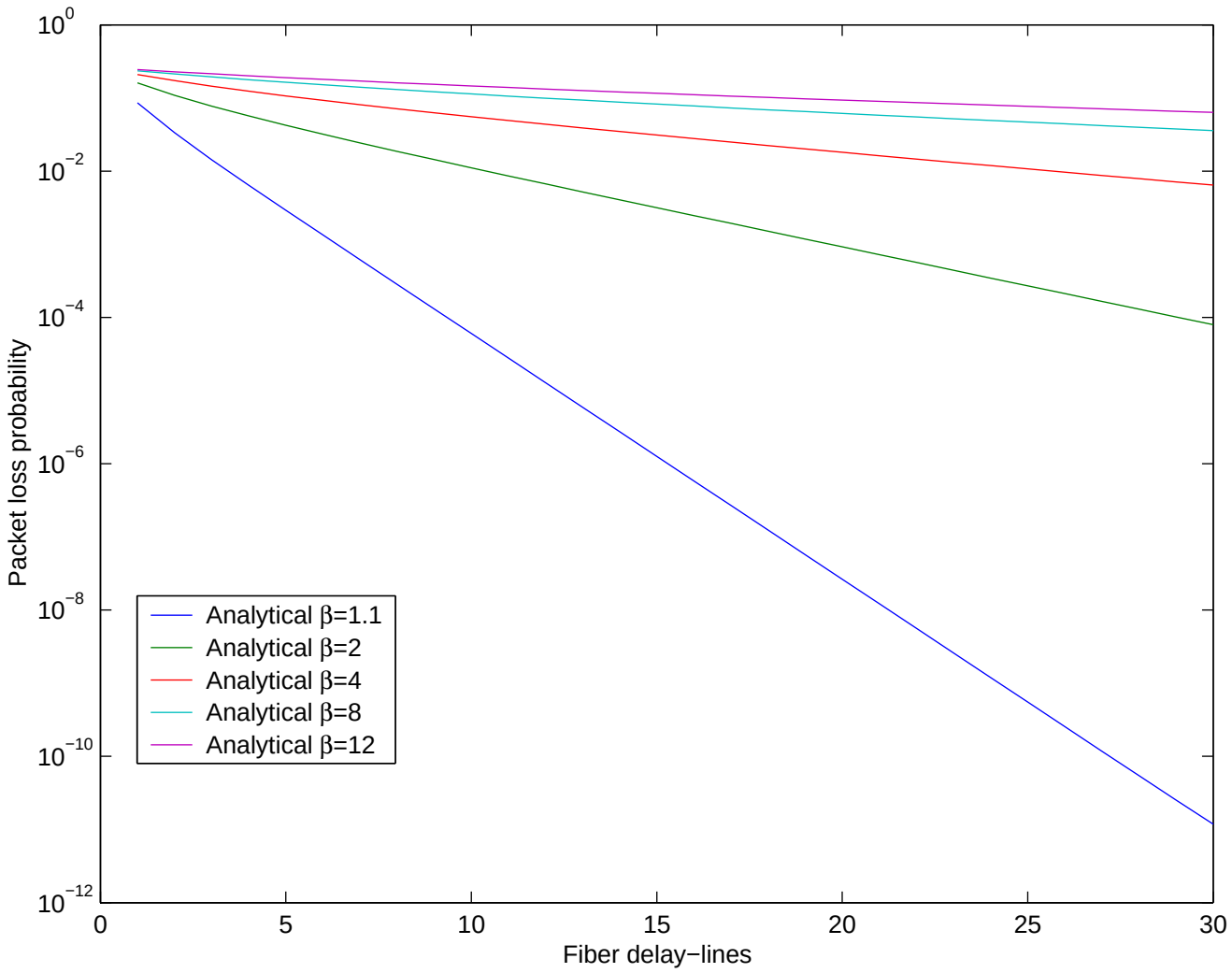

Figure 12: Packet Loss Probability versus buffer depth using burstiness as a variable parameter: load per channel 0.8.

References

[1] T-C. Hou, and A. K. Wong, "Queueing Analysis for ATM Switching of Mixed Continuous-Bit-Rate and Bursty Traffic", *In Proc. INFOCOM90*, Vol..2, pp. 660-667, 1990.
Base de datos de Biblioteca Digital: IEEE Explore

[2] A. Borella, F. Chiaraluce, F. Meschini, , "Statistical Multiplexing of Random Process in Packet Switching Networks", *IEE, Proc. Commun.* Vol. 143. No 5, pp. 325-334, Oct. 1996.
Base de datos de Biblioteca Digital: IEEE Explore

[3] S. L. Danielsen, B. Mikkelsen, C. Joergensen, T. Durhuus, K. E. Stubkjaer, "WDM packet switch architectures and analysis of the influence of tuneable wavelength converters on the

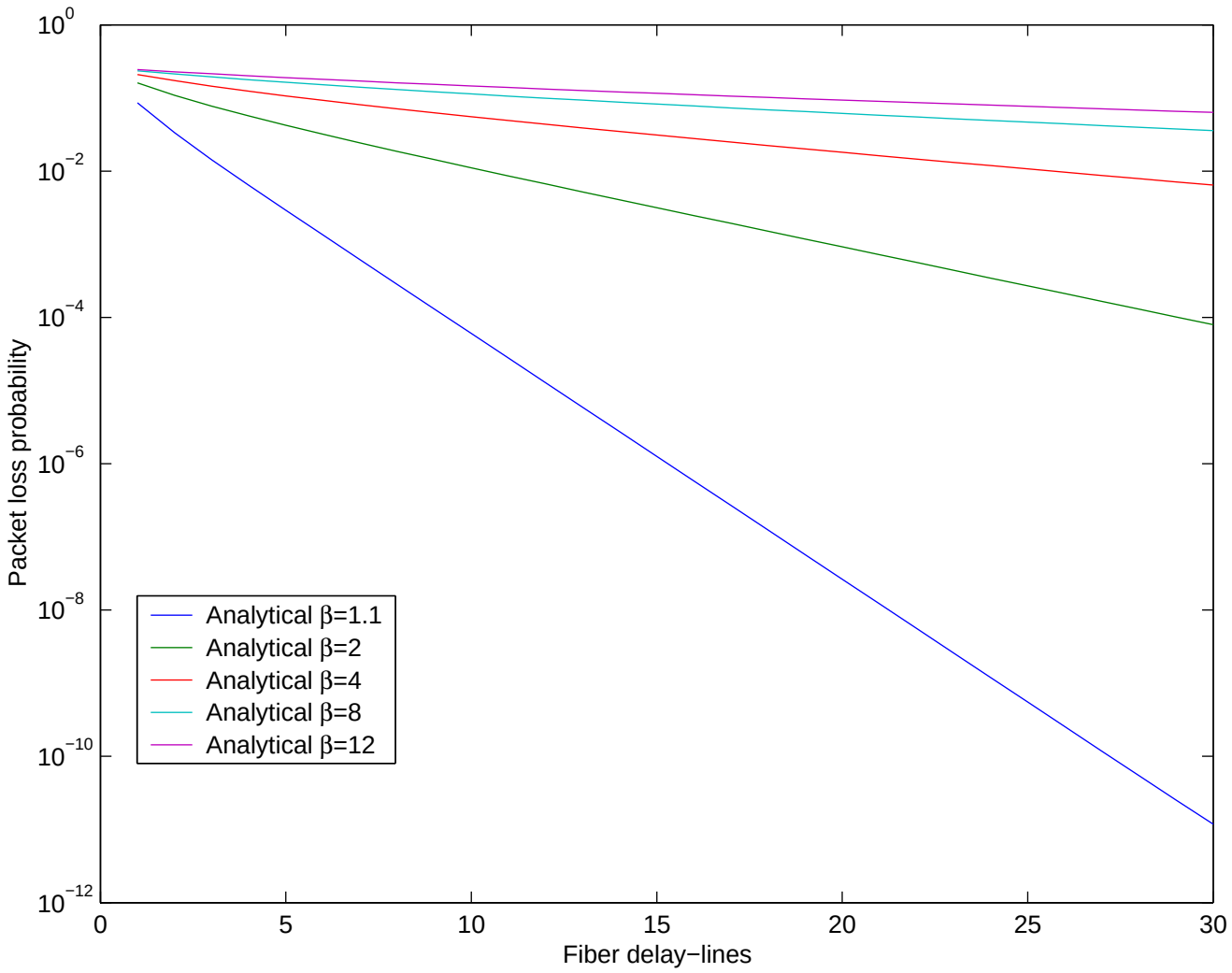

Figure 12: Packet Loss Probability versus buffer depth using burstiness as a variable parameter: load per channel 0.8.

References

[1] T-C. Hou, and A. K. Wong, "Queueing Analysis for ATM Switching of Mixed Continuous-Bit-Rate and Bursty Traffic", *In Proc. INFOCOM90*, Vol..2, pp. 660-667, 1990.
Base de datos de Biblioteca Digital: IEEE Explore

[2] A. Borella, F. Chiaraluce, F. Meschini, , "Statistical Multiplexing of Random Process in Packet Switching Networks", *IEE, Proc. Commun.* Vol. 143. No 5, pp. 325-334, Oct. 1996.
Base de datos de Biblioteca Digital: IEEE Explore

[3] S. L. Danielsen, B. Mikkelsen, C. Joergensen, T. Durhuus, K. E. Stubkjaer, "WDM packet switch architectures and analysis of the influence of tuneable wavelength converters on the

performance", *J. Lightwave Technol.*, vol. 15, pp. 219-226, Feb. 1997.
Base de datos de Biblioteca Digital: IEEE Explore

[4] S. L. Danielsen, C. Joergensen, B. Mikkelsen, K. E. Stubkjaer, "Optical packet switched network layer without optical buffers", *IEEE Photon. Technol. Lett.*, vol. 10, pp. 896-898, June 1998.
Base de datos de Biblioteca Digital: IEEE Explore

[5] W. E. Leland, M. S. Taqqu, W. Willinger, D. V. Wilson, "On the Self-Similar Nature of Ethernet Traffic (Extended Version)", *IEEE/ACM Transactions on Networking*, vol. 2, No. 1, February 1994.
Base de datos de Biblioteca Digital: IEEE Explore

[6] R. Nelson, *Probability Stochastic Processes, and Queueing Theory*, Spring-Verlang, New York, 1995.

[7] A. León-García, *Probability and Random Processes for Electrical Engineering*, 2nd Ed. Addison Wesley, 1994

[8] A. Papoulis, *Probability, random variables, and stochastic process*, 2nd edition, Mc- Graw Hill, 1984.

[9] J. Beran, *Statistics for long-memory processes*, Chapman and Hall, New York, 1994

[10] R. Jain and S. Routhier, "Packet trains-measurements and a new model for computer network traffic", *IEEE J. Select. Areas Commun.*, Vol..4, No. 6, 986995, Jun.1986.
Base de datos de Biblioteca Digital: IEEE Explore

[11] W. E. Leland, and D. V. Wilson, "High Time Resolution Measurements and Analysis of LAN Traffic: Implications for LAN Interconnection", *Proc. INFOCOM91*, vol.3, pp. 1360-1366,1991.
Base de datos de Biblioteca Digital: IEEE Explore

[12] J. Shaikh, J. Rexford, and K. Shin, "Load-sensitive routing of long-lived IP flows", *In Proc. ACM SIGCOMM99*, pp. 215226, 1999.

[13] K. Park and W. Willinger, *Self-similar network traffic: an overview, in self-similar network traffic and performance evaluation*, Ch. 1, edited by K. Park and W. Willinger, Wiley, 2000.

[14] V. Paxson and S. Floyd, "Wide-area traffic: the failure of Poisson modeling", *IEEE/ACM Transactions on Networking* 3, pp. 226-244, 1995.
Base de datos de Biblioteca Digital: IEEE Explore

[15] H. Heffes and D. M. Lucantoni, "A Markov modulated characterization of packetzed voice and data traffic and reated statistical multiplexer performance', *IEEE Journal on Selected Areas in Comm.*, Vol. SAC-4, No. 6, pp. 856-867, Sep. 1986.
Base de datos de Biblioteca Digital: IEEE Explore

[16] H. Heffes, "A class of data traffic processes-covariance function characterization and related queuing results", *Bell system tech. journal*, Vol. 59, No. 6, pp. 897-929, July- August. 1980.

[17] I. Ide, "Superposition of interrupted poisson processes and its application to packetized voice multiplexers', *in Proc. ITC89(ITC-12)* pp1399-1405, 1989.

[18] I. Noros, J. W. Roberts, A. Simonian, and T. Virtamo, "The superposition of variable bit rate in ATM multiplexer", *IEEE Journal of Selec. Areas in Comm.*; Vol. 9, No. 3, pp. 378-387, April 1991.
Base de datos de Biblioteca Digital: IEEE Explore

[19] K. Sohraby, "On the theory of general on-off sources with applications in high-speed networks", *In Proc. INFOCOM93*, Vol. 2, pp. 401-410, 1993.
Base de datos de Biblioteca Digital: IEEE Explore

[20] I. I. Makhamreh, N. D. Georganas and D. McDonald, "Analysis of an output-buffered ATM switch with speed-up constrains under correlated and imbalanced bursty traffic", *IEE Proc. Communications* Vol. 142, No. 2, pp. 61-66, April 1995.
Base de datos de Biblioteca Digital: IEEE Explore

[21] M. G. Hluchyj, M. J. Karol, "Queueing in high-performance packet switching", *IEEE J. Select. Areas Commun.*, vol. 6, pp. 1587-1597, Dec. 1988.
Base de datos de Biblioteca Digital: IEEE Explore

[22] F. Huebner, D. Liu and J. M. Fernandez, "Queueing Performance Comparison of Traffic Models for Internet Traffic", *In Proc. of Globecom 98*, pp 471476, 1998.
Base de datos de Biblioteca Digital: IEEE Explore

[23] T. Tarongí, D., D. Rodellar, J. M. Torner, J. Solé-Pareta, S. Borgione, "Traffic characterization using optical based packet switches with Poisson and fractal traffic sources", *In Proc. ONDM 01*,. 2001

[24] K. M. Guild and M. J. O'Mahony, "Routing and buffering architecture in all-optical networks", *Electronic Letters*, vol. 35. No. 02, Jan. 1999.
Base de datos de Biblioteca Digital: IEEE Explore

[25] G. Castañón, "Asymmetric WDM all-optical packet switched routers", *In Proc. OFC'00*, paper WD-4, 2000.
Base de datos de Biblioteca Digital: IEEE Explore

[26] H. M. T. Liu, and K. Y. Lee, "The knockout switch under nonuniform traffic", *In Proc. of Globecom'88*, Vol. III. pp. 1628-1634, 1988.
Base de datos de Biblioteca Digital: IEEE Explore

A Professor and author data

Datos del professor
Nombre: Dr. Cesar Vargas Rosales
Correo electrónico: cvargas@itesm.mx
Nombre de la materia: Analisis del Desempeño de Redes
Categoría: Posgrado
Calificacion otorgada por el profesor: 100/100

Datos del autor
Nombre: Ing. Job Josué Constantino Prado
Correo electrónico: job001@hotmail.com
Matrícula: 785781
Teléfonos: (81)10530932, (443)3244684